

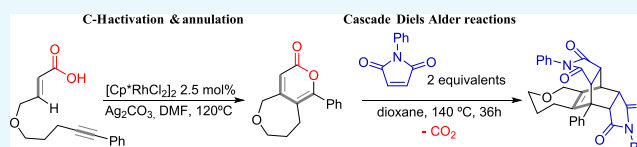
Rhodium(III)-Catalyzed Intramolecular Annulations of Acrylic and Benzoic Acids to Alkynes

David F. Fernández,[†] Noelia Casanova,[†] José Luis Mascareñas,^{*†} and Moisés Gulías^{*†}

Centro Singular de Investigación en Química Biolóxica e Materiais Moleculares (CIQUS) and Departamento de Química Orgánica, Universidade de Santiago de Compostela, 15782 Santiago de Compostela, Spain

Supporting Information

ABSTRACT: Rh(III) catalysts can promote a formal (4 + 2) intramolecular oxidative annulation between acrylic or benzoic acid derivatives and alkynes. The reaction, which involves a C–H activation process, allows for a rapid assembly of appealing bicyclic pyran-2-ones and tricyclic isocoumarin derivatives in moderate to good yields. The α -pyrone moiety of the products provides for further manipulations to obtain relatively complex cyclic skeletons in a very simple manner.



INTRODUCTION

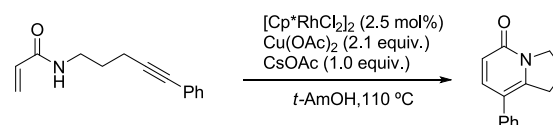
Ongoing progress in modern chemical synthesis depends on the invention of new transformations that allow a target-relevant increase in complexity without the generation of byproducts or atomic waste.¹ In this context, the functionalization of “inert” C–H bonds using transition-metal catalysis represents a particularly appealing strategy.² Most of the C–H activation reactions consist of couplings, cyclization, and halogenation or acetoxylation processes. However, in recent years, there has been an increasing number of reports on processes that couple the C–H activation with a formal cycloaddition, many of them using alkynes as reaction partners.^{3,4} These strategies represent very powerful alternatives to classical cycloadditions of unsaturated substrates and are especially attractive to ensemble heterocyclic products.⁵

One of the landmark advances in this topic consists of the annulation between benzoic or acrylic acids and alkynes to give isocoumarin or α -pyrone products. This reaction has been performed using rhodium,⁶ ruthenium,⁷ and even cobalt complexes⁸ and provides one of the simplest ways to ensemble these types of oxacyclic skeletons from simple precursors. Remarkably, despite the synthetic value of the reaction, we are not aware of the development of intramolecular variants. Tethering the alkyne to the acrylic or benzoic acid moiety would not only allow controlling the regioselectivity, which is an issue in the intermolecular processes, but also provide for a higher increase in skeletal complexity.

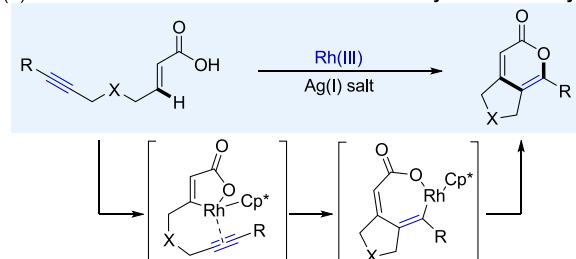
In 2013, we reported one of the first intramolecular formal annulations involving C–H activations. The reaction, shown in Scheme 1A, involved an acrylamide and a N-tethered alkyne and provided a practical entry to isoquinoline products.⁹ In the case of the acrylic acid derivatives, the alkyne must be tethered to the carbon instead of the oxygen atom of the acid. The C–H activation would generate a rhodacycle, which after migratory insertion of the alkyne and reductive elimination should produce the bicyclic lactone adducts (Scheme 1B). Noteworthy, α -pyrones and related lactones fused to other

Scheme 1. Intramolecular Annulations and Natural Products with Polycyclic Pyrone Cores

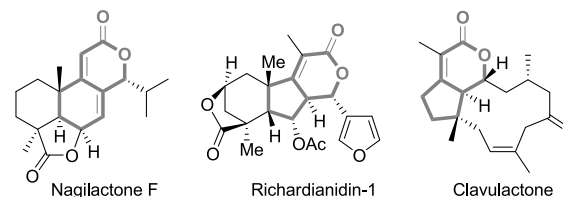
(A) Our previous work: Intramolecular annulation of acrylamides with alkynes



(B) This work: Intramolecular annulation between acrylic acid and alkynes



(C) Some polycyclic natural products with 2-pyrone cores



rings are present in many natural products (Scheme 1C) and therefore the technology might find important synthetic applications in the future.

Herein, we present the first examples of intramolecular, formal (4 + 2) annulations between acrylic acids and alkynes.¹⁰ The methodology can be extended to benzoic acids and

Received: January 3, 2019

Accepted: March 18, 2019

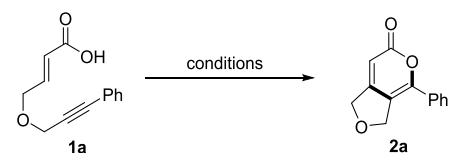
Published: April 4, 2019

pyrrole-3-carboxylic acids, providing for the assembly of interesting polycycles in just one catalytic step. Importantly, we also present preliminary examples on the manipulation potential of the resulting pyrones.

RESULTS AND DISCUSSION

The viability of the annulation was studied on precursor **1a**, readily assembled from phenylpropynol and methyl buta-2,3-dienoate (see the [Supporting Information](#)). At the outset, we were concerned about the C–H activation step, as it might be compromised by the presence of substitution in the β -carbon of the acrylic acid moiety. However, we were pleased to find that the treatment of **1a** with 2.5 mol % $[\text{Cp}^*\text{RhCl}_2]_2$ in *tert*-amyl alcohol at 100 °C, using 2 equiv of copper diacetate as oxidant, generates the desired cycloadduct, which was isolated in 50% yield (entry 1, [Table 1](#)). Using dimethylformamide

Table 1. Optimization of the Reaction Conditions^a



entry	catalyst	solvent	T (°C)	yield (%)
1 ^b	$[\text{Cp}^*\text{RhCl}_2]_2$	<i>t</i> AmOH	100	50 ^b
2 ^b	$[\text{Cp}^*\text{RhCl}_2]_2$	DMF	120	25 ^b
3	$[\text{Cp}^*\text{RhCl}_2]_2$	DMF	120	82 ^c
4	$[\text{Cp}^*\text{RhCl}_2]_2$	DCE	80	20
5	$[\text{Cp}^*\text{RhCl}_2]_2$	toluene	110	36
6	$[\text{Cp}^*\text{RhCl}_2]_2$	MeOH	60	71
7	$[(p\text{-cymene})\text{RuCl}_2]_2$	DMF	120	28
8	$[\text{Cp}^*\text{IrCl}_2]_2$	DMF	120	
9	$[\text{Cp}^*\text{Rh}(\text{CH}_3\text{CN})_3](\text{SbF}_6)_2$	DMF	120	21 ^{c,d}
10	$[\text{Cp}^*\text{RhCl}_2]_2$	DMF	120	31 ^e

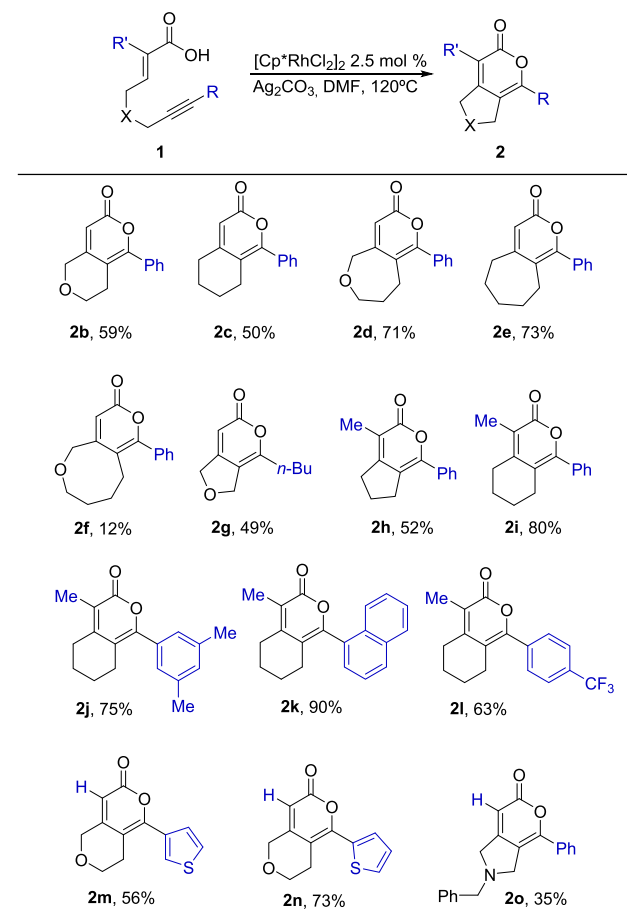
^aReaction conditions: 0.20 mmol of **1a**, catalyst (2.5 mol %), 2 equiv of Ag_2CO_3 , solvent (0.8 mL), 12 h. Yields determined by internal standard. ^b $\text{Cu}(\text{OAc})_2 \cdot \text{H}_2\text{O}$ (2 equiv) instead of Ag_2CO_3 . ^cIsolated yield. ^d5 mol % of catalyst. ^e1 equiv of Ag_2CO_3 .

(DMF) as solvent, the yield was lower (entry 2); however, switching the oxidant to silver carbonate, we obtained the expected pyrone **2a** in 82% yield (entry 3).

With other solvents, such as 1,2-dichloroethane, toluene, or MeOH, we observed poorer conversions. Interestingly, using $[(p\text{-cymene})\text{RuCl}_2]_2$ as catalyst, which had been previously used in intermolecular annulations, the yield was modest (entry 7), whereas with $[\text{Cp}^*\text{IrCl}_2]_2$, the starting material was fully recovered (entry 8). The cationic catalyst $[\text{Cp}^*\text{Rh}(\text{CH}_3\text{CN})_3](\text{SbF}_6)_2$ also resulted in a less effective process (entry 9). The yield of the product was also lower when only 1 equiv of silver carbonate was used (entry 10).

With the optimized conditions at hand, we studied the scope with other precursors (see [Table 2](#)). The reaction is also efficient with acrylic acid derivatives featuring longer connecting tethers and therefore products with 6- and 7-membered rings containing either a fully carbon chain or an ether were obtained in good yields (**2b–e**, 50–73%). Further enlarging the connection slows down the reaction and thus the 8-membered product **2f** was isolated in low yield (12%). The presence of an aliphatic substituent (*n*-Bu) instead of the phenyl ring in the alkyne is tolerated, albeit the yield was slightly lower (**2g**, 49%). A methyl group in the α -position of

Table 2. Substrate Scope for Substituted Acrylic Acids^a

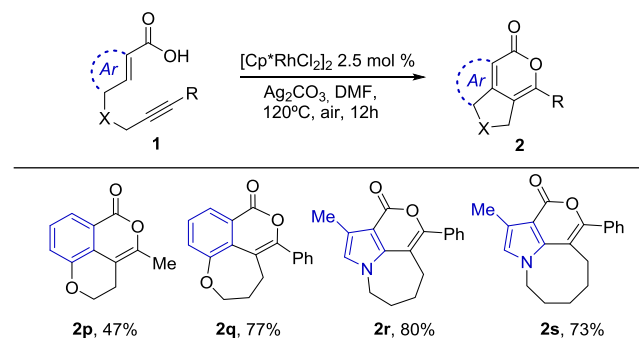


^aConditions: 50 mg of **1**, 2 equiv of Ag_2CO_3 , 2.5 mol % of $[\text{Cp}^*\text{RhCl}_2]_2$, DMF (0.3 M), 120 °C, 12 h. Isolated yields.

the acrylic acids does not compromise the reaction, and the expected adducts were obtained in good yields (**2h** and **2i**, 52–80%). We also found that the reaction is efficient with substrates containing other aromatic substituents at the alkyne, with either electron-rich (**2j** and **2k**, 75 and 90% yield) or electron-deficient groups (**2l**, 63% yield), as well as for heteroaromatic substituents (**2m** and **2n**, 56 and 73% yield). We have also tested the reaction in a precursor bearing a nitrogen atom in the connecting tether. The reaction worked, but the product **2o** was isolated in lower yield.

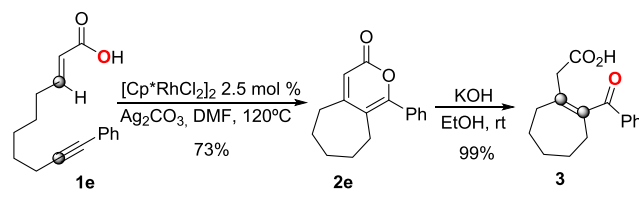
At this point, we also assayed the reaction with benzoic instead of acrylic acid derivatives. These precursors were readily synthesized from commercially available products in one or two steps (see the [Supporting Information](#)). Using the same conditions as above, we obtained the expected products **2p** and **2q**, featuring 6- and 7-membered rings in 47 and 77% yields, respectively ([Table 3](#)). Interestingly, we also demonstrated that *N*-alkyl 3-carboxy pyrroles **1r** and **1s** participate in the process to give the corresponding adducts **2r** and **2s** featuring seven- and eight-membered rings in excellent yields (80 and 73% respectively). Pyrrole-fused polycyclic products are present in many natural compounds and therefore this methodology might provide an easy way to generate these types of structures.

Although the above cycloadducts are of intrinsic interest, we envisioned that the pyrone structure might allow designed manipulations to obtain other relevant scaffolds. Therefore, the

Table 3. Scope for Aromatic Substrates^a

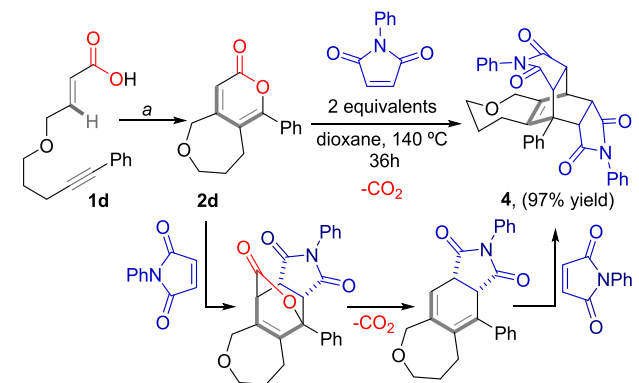
^aConditions: 50 mg of **1**, 2 equiv of Ag_2CO_3 , 2.5 mol % of $[\text{Cp}^*\text{RhCl}_2]_2$, DMF (0.3 M), 120°C , 12 h. Isolated yields.

treatment of product **2e** with potassium hydroxide in ethanol at room temperature promoted a quantitative conversion to the keto-carboxylic acid **3**. Formally, the transformation of **1e** to **3** can be visualized as a cyclization/hydration process, something that does not seem to be easy to achieve using alternative technologies (Scheme 2).¹¹

Scheme 2. Hydrolysis of the α -Pyrone

Moreover, the presence of a *cis*-diene in pyrone adducts suggested the possibility of performing Diels–Alder cycloadditions. Remarkably, the treatment of pyrone **2d**, prepared in a 2 mmol scale from **1d**, with 2 equiv of *N*-phenylmaleimide at 140°C produced bis-adduct **4** in good yield and complete stereoselectivity. The structure of this pentacyclic adduct was confirmed by X-ray diffraction crystallography (see Scheme 3 and Figure 1).

This surprising transformation can be explained in terms of a cascade process involving several Diels–Alder reactions.¹² An initial (4 + 2) Diels–Alder cycloaddition, even between

Scheme 3. Cascade Diels–Alder Processes^a

^aConditions: (a) 2.05 mmol of **1d**, 1.5 equiv of Ag_2CO_3 , 2.5 mol % of $[\text{Cp}^*\text{RhCl}_2]_2$, DMF (10.2 mL, 0.2 M), 120°C , 24 h, 77% yield.

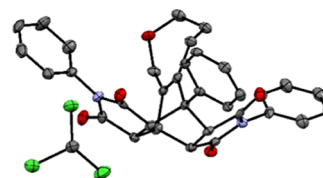


Figure 1. X-ray structure of cycloadduct **4**. Hydrogens omitted for clarity.

electron-deficient partners, is followed by a retro-cycloaddition with concomitant extrusion of carbon dioxide. Finally, the resulting intermediate reacts with another equivalent of maleimide through a second Diels–Alder to form the polycyclic structure. Overall, the transformation of **1d** into **4** (two steps) conveys the formation of five carbon–carbon bonds and five cycles, therefore providing for an impressive increase in complexity with total atom economy.

CONCLUSIONS

In summary, we have developed the first examples of intramolecular (4 + 2) annulations between acrylic acids and alkynes. The oxidative annulation is promoted by Rh(III) catalysts and allows for the straightforward assembly of bicyclic and tricyclic pyrone-containing adducts from simple precursors. We also presented preliminary demonstrations of relevant manipulations of the cycloadducts, including a remarkable thermal cycloaddition cascade in the presence of an electron-poor dienophile.

EXPERIMENTAL SECTION

General Comments. Dry solvents were freshly distilled under argon from an appropriate drying agent before use. Dried *N,N*-dimethylformamide was purchased from Sigma-Aldrich and used without further purification. $[\text{RhCp}^*\text{Cl}_2]_2$ (99%) [12354-85-7] and Ag_2CO_3 (99%) [534-16-7] were purchased from Sigma-Aldrich. All other chemicals were purchased from Sigma-Aldrich, TCI, Alfa Aesar, and Strem-Chemicals and used without further purification. All reactions dealing with air and moisture-sensitive compounds were carried out in an oven-dried reaction flask under an argon atmosphere with dry solvents. The abbreviation “rt” refers to reactions carried out approximately at 23°C . Reaction mixtures were stirred using Teflon-coated magnetic stirring bars. Reaction temperatures were maintained using Thermo-watch-controlled silicone oil baths. Thin-layer chromatography (TLC) was performed on silica gel plates, and components were visualized by observation under UV light and/or by treating the plates with *p*-anisaldehyde or phosphomolybdic acid solutions, followed by heating. Flash chromatography was carried out on silica gel unless otherwise stated. Drying was performed with anhydrous Na_2SO_4 or MgSO_4 . Concentration refers to the removal of volatile solvents via distillation using a Büchi rotary evaporator followed by residual solvent removal under high vacuum. Melting points (mp) were determined with an M-560 BÜCHI apparatus. NMR spectra were recorded in CDCl_3 at 300 MHz (Varian), unless other solvents are specified. Carbon types and structural assignments were determined from distortionless enhancement by polarization transfer-NMR. NMR spectra were analyzed using MestreNova NMR data processing software (www.mestrelab.com). 1,3,5-Trimethoxybenzene was used as internal standard. The following abbreviations are used to indicate signal multiplicity:

s, singlet; d, doublet; t, triplet; q, quartet; dd, double doublet; ddd, doublet of doublet of doublets; td, triple doublet; dt, doublet of triplets; dq, doublet of quartet; m, multiplet; brs, broad singlet. Electrospray ionization mass spectra (ESI-MS) were acquired using an IT-MS Bruker Amazon SL at CIQUS and also using chemical ionization (CI) electron impact (EI), electrospray ionization (ESI), or atmospheric-pressure chemical ionization (APCI) at the CACTUS facility of the University of Santiago de Compostela. The reactions were monitored by TLC.

General Procedure for the Annulation Reaction. An oven-dried Schlenk tube equipped with a septum and magnetic stirring bar was charged with acrylic or benzoic acid (0.23 mmol), bis(dichloro(pentamethylcyclopentadienyl)rhodium) (2.5 mol %), silver carbonate (0.46 mmol), and DMF (0.8 mL). The reaction mixture was then stirred at 120 °C. After 24 h, the reaction mixture was concentrated in vacuum. Purification of the crude product was done by flash chromatography on silica gel (1:10–1:3 EtOAc/hexane).

4-Phenyl-3H-furo[3,4-c]pyran-6(1H)-one (2a). Dark-yellow solid, mp 117–118 °C (41 mg, 82%). ¹H NMR (300 MHz, CDCl₃): δ 7.65–7.57 (m, 2H), 7.53–7.45 (m, 3H), 6.19–6.12 (m, 1H), 5.09 (s, 2H), 4.87 (d, *J* = 1.6 Hz, 2H). ¹³C NMR (75 MHz, CDCl₃): δ 162.7 (C), 161.1 (C), 152.4 (C), 131.4 (C), 130.8 (CH), 129.1 (CH), 126.6 (CH), 116.1 (C), 104.4 (CH), 70.9 (CH₂), 70.1 (CH₂). High-resolution mass spectroscopy (HRMS) (EI-FIA-TOF): *m/z* calculated for C₁₃H₁₀O₃ ([M]⁺) 214.0630, found 214.0636.

1-Phenyl-7,8-dihydropyrano[4,3-c]pyran-3(5H)-one (2b). White solid, mp 128–129 °C (29.5 mg, 59%). ¹H NMR (300 MHz, CDCl₃): δ 7.65–7.59 (m, 2H), 7.49–7.45 (m, 2H), 7.34–7.30 (m, 1H), 6.01 (s, 1H), 4.67 (d, *J* = 1.4 Hz, 2H), 3.83 (t, *J* = 5.7 Hz, 2H), 2.77 (t, *J* = 5.6 Hz, 2H). ¹³C NMR (75 MHz, CDCl₃): δ 161.8 (CO), 154.6 (C), 130.4 (CH), 128.7 (CH), 128.6 (CH), 125.6 (C), 124.3 (C), 109.9 (C), 107.8 (CH), 67.3 (CH₂), 65.5 (CH₂), 25.3 (CH₂). HRMS (ESI-FIA-TOF): *m/z* calculated for C₁₄H₁₃O₃ ([M + H]⁺) 229.0857, found 229.0857.

1-Phenyl-5,6,7,8-tetrahydro-3H-isochromen-3-one (2c). Light-yellow solid, mp 113–114 °C (25 mg, 50%). ¹H NMR (300 MHz, CDCl₃): δ 7.60–7.51 (m, 2H), 7.47–7.38 (m, 3H), 6.08 (s, 1H), 2.70 (t, *J* = 5.9 Hz, 2H), 2.60 (t, *J* = 6.2 Hz, 2H), 1.82–1.61 (m, 4H). ¹³C NMR (75 MHz, CDCl₃): δ 162.5 (C), 158.5 (C), 156.8 (C), 132.6 (C), 129.8 (CH), 128.9 (CH), 128.3 (CH), 114.0 (C), 111.4 (CH), 29.7 (CH₂), 25.3 (CH₂), 22.7 (CH₂), 21.6 (CH₂). Low-resolution mass spectrometry (LRMS) (*m/z*, CI) 227.2 ([M+H]⁺, 100), 213.2 (54), 199.2 (23), 105.1 (52). HRMS (EI-FIA-TOF): *m/z* calculated for C₁₅H₁₄O₂ ([M]⁺) 226.0994, found 226.0980.

1-Phenyl-8,9-dihydro-7H-pyrano[4,3-c]oxepin-3(5H)-one (2d). White solid, mp 91–92 °C (35.5 mg, 71%). ¹H NMR (300 MHz, CDCl₃): δ 7.47–7.35 (m, 5H), 6.11 (s, 1H), 4.40 (s, 2H), 3.88 (t, *J* = 5.1 Hz, 2H), 2.78–2.69 (m, 2H), 1.78 (p, *J* = 5.2 Hz, 2H). ¹³C NMR (75 MHz, CDCl₃): δ 161.9 (C), 158.0 (C), 157.6 (C), 132.4 (C), 129.9 (CH), 128.9 (CH), 128.4 (CH), 116.8 (C), 112.5 (CH), 74.9 (CH₂), 73.5 (CH₂), 30.9 (CH₂), 27.6 (CH₂). HRMS (ESI-FIA-TOF): *m/z* calculated for C₁₅H₁₃O₃ ([M + H]⁺) 243.1016, found 243.1016.

1-Phenyl-6,7,8,9-tetrahydrocyclohepta[c]pyran-3(5H)-one (2e). White solid, mp 74–77 °C (36.5 mg, 73%). ¹H NMR (300 MHz, CDCl₃): δ 7.50–7.39 (m, 5H), 6.11 (s, 1H), 2.68–2.62 (m, 2H), 2.60–2.54 (m, 2H), 1.80–1.63 (m, 6H). ¹³C

NMR (75 MHz, CDCl₃): δ 163.4 (C), 162.7 (C), 157.0 (C), 133.0 (C), 129.7 (CH), 129.1 (CH), 128.4 (CH), 118.9 (C), 111.9 (CH), 36.5 (CH₂), 31.3 (CH₂), 29.3 (CH₂), 28.3 (CH₂), 28.3 (CH₂). HRMS (APCI-FIA-TOF): *m/z* calculated for C₁₆H₁₇O₂ ([M + H]⁺) 241.1223, found 241.1223.

1-Phenyl-7,8,9,10-tetrahydropyrano[4,3-c]oxocin-3(5H)-one (2f). Yellowish solid, mp 118–120 °C (6 mg, 12%). ¹H NMR (300 MHz, CDCl₃): δ 7.53–7.40 (m, 5H), 6.14–6.07 (m, 1H), 4.69–4.62 (m, 2H), 3.86 (t, *J* = 4.9 Hz, 2H), 2.88 (t, *J* = 6.3 Hz, 2H), 1.81–1.64 (m, 4H). ¹³C NMR (75 MHz, CDCl₃): δ 162.1 (C), 160.4 (C), 159.4 (C), 133.141 (C), 130.1 (CH), 129.1 (CH), 128.6 (CH), 115.8 (C), 110.4 (CH), 72.6 (CH₂), 71.4 (CH₂), 27.9 (CH₂), 25.5 (CH₂), 25.3 (CH₂). LRMS (*m/z*, CI) 257.1 ([M+H]⁺, 100), 229.1 (6). HRMS (EI-FIA-TOF): *m/z* calculated for C₁₆H₁₆O₃ ([M]⁺) 256.1099, found 256.1094.

4-Butyl-3H-furo[3,4-c]pyran-6(1H)-one (2g). Viscous yellow oil (24.5 mg, 49%). ¹H NMR (300 MHz, CDCl₃): δ 6.01–6.00 (m, 1H), 4.81–4.79 (m, 1H), 4.79–4.77 (m, 1H), 2.42 (t, *J* = 7.5 Hz, 2H), 1.75–1.61 (m, 2H), 1.46–1.16 (m, 2H), 0.93 (t, *J* = 7.3 Hz, 3H). ¹³C NMR (75 MHz, CDCl₃): δ 163.3 (C), 160.5 (C), 157.7 (C), 116.3 (C), 103.5 (CH), 71.3 (CH₂), 68.63 (CH₂), 32.38 (CH₂), 28.72 (CH₂), 22.30 (CH₂), 13.7 (CH₃). HRMS (QI): *m/z* calculated for C₁₁H₁₅O₃ ([M + H]⁺) 195.1021, found 195.1026.

4-Methyl-1-phenyl-6,7-dihydrocyclopenta[c]pyran-3(5H)-one (2h). Reddish solid (26 mg, 52%). ¹H NMR (300 MHz, CDCl₃): δ 7.77–7.66 (m, 2H), 7.49–7.33 (m, 3H), 2.95 (t, *J* = 7.3 Hz, 2H), 2.74 (t, *J* = 7.5 Hz, 2H), 2.14–2.00 (m, 5H). ¹³C NMR (75 MHz, CDCl₃): δ 164.2 (C), 160.7 (C), 150.4 (C), 132.7 (C), 129.4 (CH), 128.6 (CH), 127.0 (CH), 120.1 (C), 116.8 (C), 31.5 (CH₂), 30.7 (CH₂), 25.7 (CH₂), 13.3 (CH₃). LRMS (*m/z*, CI) 227.0 ([M+H]⁺, 100), 199.0 (10). HRMS (EI-FIA-TOF): *m/z* calculated for C₁₅H₁₄O₂ ([M]⁺) 226.0994, found 226.0995.

4-Methyl-1-phenyl-5,6,7,8-tetrahydro-3H-isochromen-3-one (2i). Light-yellow solid, mp 84–87 °C (40 mg, 80%). ¹H NMR (300 MHz, CDCl₃): δ 7.57–7.51 (m, 2H), 7.45–7.38 (m, 3H), 2.68–2.55 (m, 4H), 2.07 (s, 3H), 1.84–1.74 (m, 2H), 1.66–1.58 (m, 2H). ¹³C NMR (75 MHz, CDCl₃): δ 163.7 (C), 153.8 (C), 151.9 (C), 133.0 (C), 129.6 (CH), 129.1 (CH), 128.4 (CH), 119.8 (C), 114.0 (C), 27.7 (CH₂), 26.2 (CH₂), 22.4 (CH₂), 22.0 (CH₂), 12.1 (CH₃). LRMS (*m/z*, CI) 241.1 ([M+H]⁺, 100), 213.1 (14). HRMS calculated for C₁₆H₁₆O₂ 240.1150, found 240.1147. HRMS (EI-FIA-TOF): *m/z* calculated for C₁₆H₁₆O₂ ([M]⁺) 240.1150, found 240.1147.

1-(3,5-Dimethylphenyl)-4-methyl-5,6,7,8-tetrahydro-3H-isochromen-3-one (2j). Reddish solid (37.5 mg, 75%). ¹H NMR (300 MHz, CDCl₃): δ 7.08 (s, 2H), 6.95 (s, 1H), 2.66–2.40 (m, 4H), 2.26 (s, 6H), 1.99 (s, 3H), 1.79–1.63 (m, 2H), 1.62–1.44 (m, 2H). ¹³C NMR (75 MHz, CDCl₃): δ 163.7 (C), 154.0 (C), 152.0 (C), 137.8 (C), 132.6 (C), 131.1 (CH), 126.7 (CH), 119.2 (C), 113.7 (C), 27.8 (CH₂), 26.3 (CH₂), 22.4 (CH₂), 22.1 (CH₂), 21.4 (CH₃), 12.1 (CH₃). HRMS (EI-FIA-TOF): *m/z* calculated for C₁₈H₂₀O₂ ([M]⁺) 268.1463, found 268.1470.

4-Methyl-1-(naphthalen-1-yl)-5,6,7,8-tetrahydro-3H-isochromen-3-one (2k). Yellow solid, mp 94–96 °C (45 mg, 90%). ¹H NMR (300 MHz, CDCl₃): δ 7.97–7.84 (m, 2H), 7.75–7.64 (m, 1H), 7.57–7.43 (m, 4H), 2.69 (t, *J* = 7.7 Hz, 2H), 2.21 (t, *J* = 6.4 Hz, 2H), 2.13 (s, 3H), 1.83–1.72 (m, 2H), 1.62–1.50 (m, 2H). ¹³C NMR (75 MHz, CDCl₃): δ

163.9 (C), 153.5 (C), 151.7 (C), 133.8 (C), 131.3 (C), 130.5 (C), 130.2 (CH), 128.7 (CH), 128.2 (CH), 127.1 (CH), 126.4 (CH), 125.3 (CH), 125.2 (CH), 120.1 (C), 115.5 (C), 27.7 (CH₂), 25.1 (CH₂), 22.1 (CH₂), 22.1 (CH₂), 12.1 (CH₃). HRMS (EI-FIA-TOF): *m/z* calculated for C₂₀H₁₈O₂ ([M]⁺) 290.1307, found 290.1310.

4-Methyl-1-(4-(trifluoromethyl)phenyl)-5,6,7,8-tetrahydro-3H-isochromen-3-one (2l). Yellow solid, mp 134–135 °C (31.5 mg, 63%). ¹H NMR (300 MHz, CDCl₃): δ 7.69–7.66 (m, 4H), 2.69–2.55 (m, 4H), 2.12–2.06 (m, 3H), 1.87–1.72 (m, 2H), 1.71–1.57 (m, 2H). ¹³C NMR (75 MHz, CDCl₃): δ 163.2 (C), 151.9 (C), 151.6 (C), 136.4 (C), 131.4 (C, q, *J* = 32.3 Hz), 129.5 (CH), 125.4 (CH, q, *J* = 3.7 Hz), 124.0 (CF₃, q, *J* = 272.6 Hz), 120.9 (C), 115.0 (C), 27.7 (CH₂), 26.1 (CH₂), 22.3 (CH₂), 21.9 (CH₂), 12.2 (CH₃). HRMS (EI-FIA-TOF): *m/z* calculated for C₁₇H₁₅F₃O₂ ([M]⁺) 308.1024, found 308.1006.

1-(Thiophen-3-yl)-7,8-dihydropyrano[4,3-*c*]pyran-3(5H)-one (2m). Yellow solid (39.2 mg, 56%), mp 116–117 °C. ¹H NMR (300 MHz, CDCl₃): δ 7.75 (dd, *J* = 3.0, 1.3 Hz, 1H), 7.49 (dd, *J* = 5.2, 1.3 Hz, 1H), 7.40 (dd, *J* = 5.1, 2.9 Hz, 1H), 5.97–5.90 (m, 1H), 4.62 (d, *J* = 1.6 Hz, 2H), 3.88 (t, *J* = 5.8 Hz, 2H), 2.81 (t, *J* = 5.8 Hz, 2H). ¹³C NMR (75 MHz, CDCl₃): δ 161.4 (C), 154.6 (C), 153.7 (C), 133.3 (C), 127.7 (CH), 127.1 (CH), 126.2 (CH), 109.0 (C), 107.2 (CH), 67.4 (CH₂), 65.3 (CH₂), 25.2 (CH₂). HRMS (APCI-FIA-TOF): *m/z* calculated for C₁₂H₁₁O₃S ([M + H]⁺) 235.0424, found 235.0423.

1-(Thiophen-2-yl)-7,8-dihydropyrano[4,3-*c*]pyran-3(5H)-one (2n). Yellow solid (51.1 mg, 73%), mp 142–143 °C. ¹H NMR (300 MHz, CDCl₃): δ 7.63 (dd, *J* = 3.9, 1.0 Hz, 1H), 7.55 (dd, *J* = 5.1, 1.1 Hz, 1H), 7.16 (dd, *J* = 5.1, 3.8 Hz, 1H), 5.91 (s, 1H), 4.61 (d, *J* = 1.5 Hz, 2H), 3.94 (t, *J* = 5.9 Hz, 2H), 2.83 (t, *J* = 5.9 Hz, 2H). ¹³C NMR (75 MHz, CDCl₃): δ 160.8 (C), 154.5 (C), 152.9 (C), 134.3 (C), 129.9 (CH), 129.6 (CH), 128.0 (CH), 108.3 (C), 107.0 (CH), 67.6 (CH₂), 65.2 (CH₂), 25.0 (CH₂). HRMS (APCI-FIA-TOF): *m/z* calculated for C₁₂H₁₁O₃S ([M + H]⁺) 235.0422, found 235.0423.

2-Benzyl-4-phenyl-2,3-dihydropyrano[3,4-*c*]pyrrol-6(1H)-one (2o). Yellow amorphous solid (17.5 mg, 35%). ¹H NMR (300 MHz, CDCl₃): δ 7.67–7.58 (m, 2H), 7.50–7.39 (m, 3H), 7.38–7.28 (m, 5H), 6.12 (s, 1H), 3.94 (s, 2H), 3.88 (s, 2H), 3.73 (s, 2H). ¹³C NMR (75 MHz, CDCl₃): δ 162.63 (C), 161.5 (C), 137.9 (C), 131.8 (C), 130.5 (CH), 128.9 (CH), 128.8 (CH), 128.7 (C), 128.7 (CH), 127.7 (CH), 127.0 (CH), 116.9 (C), 106.1 (CH), 59.9 (CH₂), 57.3 (CH₂), 55.8 (CH₂). HRMS (APCI-FIA-TOF): *m/z* calculated for C₂₀H₁₈NO₂ ([M + H]⁺) 304.1329, found 304.1332.

4-Methyl-2,3-dihydro-6H-pyrano[3,4,5-*de*]chromen-6-one (2p). White solid, mp 161–162 °C (23.5 mg, 47%). ¹H NMR (300 MHz, CDCl₃): δ 7.7 (d, *J* = 7.8 Hz, 1H), 7.2 (t, *J* = 7.9 Hz, 1H), 7.1 (d, *J* = 8.0 Hz, 1H), 4.2 (t, *J* = 5.7 Hz, 2H), 2.7 (t, *J* = 5.8 Hz, 2H), 2.1 (s, 3H). ¹³C NMR (75 MHz, CDCl₃): δ 162.2 (C), 152.0 (C), 147.5 (C), 128.1 (CH), 124.1 (C), 121.6 (CH), 120.9 (CH), 120.4 (C), 104.0 (C), 65.8 (CH₂), 23.9 (CH₂), 15.9 (CH₃). HRMS (APCI-FIA-TOF): *m/z* calculated for C₁₂H₁₁O₃ ([M + H]⁺) 202.0700, found 202.0703.

5-Phenyl-3,4-dihydro-2H,7H-oxepino[4,3,2-*de*]isochromen-7-one (2q). White solid, mp 155–156 °C (38.5 mg, 77%). ¹H NMR (300 MHz, CDCl₃): δ 7.96 (dd, *J* = 7.5, 1.7 Hz, 1H), 7.53–7.47 (m, 2H), 7.40–7.33 (m, 3H), 7.32–7.22 (m, 2H), 4.27 (t, *J* = 6.8 Hz, 2H), 2.86 (t, *J* = 6.4 Hz,

2H), 2.12 (p, *J* = 6.7 Hz, 2H). ¹³C NMR (75 MHz, CDCl₃): δ 162.1 (C), 158.6 (C), 150.2 (C), 133.0 (C), 131.1 (C), 129.7 (CH), 129.2 (CH), 128.8 (CH), 128.5 (CH), 126.4 (CH), 124.3 (CH), 122.9 (C), 111.9 (C), 73.5 (CH₂), 29.2 (CH₂), 25.9 (CH₂). HRMS (APCI-FIA-TOF): *m/z* calculated for C₁₈H₁₅O₃ ([M + H]⁺) 279.1016, found 279.1016.

2-Methyl-5-phenyl-6,7,8,9-tetrahydro-3H-4-oxa-9a-azabenzoc[cd]azulen-3-one (2r). Yellowish solid, mp 193–194 °C (40 mg, 80%). ¹H NMR (300 MHz, CDCl₃): δ 7.52–7.46 (m, 2H), 7.43–7.34 (m, 3H), 6.50 (s, 1H), 4.16–4.10 (m, 2H), 2.89–2.81 (m, 2H), 2.36 (s, 3H), 2.11 (p, *J* = 6.6 Hz, 2H), 1.93 (p, *J* = 6.8 Hz, 2H). ¹³C NMR (75 MHz, CDCl₃): δ 160.6 (C), 151.0 (C), 140.8 (C), 133.3 (C), 129.2 (CH), 128.9 (CH), 128.2 (CH), 124.8 (CH), 118.0 (C), 109.0 (C), 108.6 (C), 47.2 (CH₂), 27.6 (CH₂), 25.3 (CH₂), 25.1 (CH₂), 10.7 (CH₃). HRMS (APCI-FIA-TOF): *m/z* calculated for C₁₈H₁₈NO₂ ([M + H]⁺) 280.1340, found 280.1332.

2-Methyl-5-phenyl-7,8,9,10-tetrahydro-3H,6H-4-oxa-10a-azacycloocta[cd]indolen-3-one (2s). Light orange solid, mp 216–217 °C (36.5 mg, 73%). ¹H NMR (300 MHz, CDCl₃): δ 7.48–7.41 (m, 2H), 7.41–7.34 (m, 3H), 6.46 (s, 1H), 4.33–4.21 (m, 2H), 2.84 (t, *J* = 7.1 Hz, 2H), 2.38 (s, 3H), 1.95–1.76 (m, 4H), 1.58–1.46 (m, 2H). ¹³C NMR (75 MHz, CDCl₃): δ 160.6 (C), 152.2 (C), 140.5 (C), 133.6 (C), 129.0 (CH), 129.0 (CH), 128.2 (CH), 125.2 (CH), 117.9 (C), 108.2 (C), 107.6 (C), 47.9 (CH₂), 30.1 (CH₂), 28.4 (CH₂), 25.4 (CH₂), 21.3 (CH₂), 10.8 (CH₃). HRMS (APCI-FIA-TOF): *m/z* calculated for C₁₉H₂₀NO₂ ([M + H]⁺) 294.1488, found 294.1489.

Synthesis of Acid 3. To a solution of 1-phenyl-6,7,8,9-tetrahydrocyclohepta[*c*]pyran-3(5H)-one (2e) (50 mg, 0.21 mmol) in EtOH (1 mL) was added a saturated aqueous solution of KOH (93.4 mg, 1.66 mmol, 10 M), and the reaction mixture was stirred for 4 h at room temperature. The mixture was poured into an ice bath, and then the solution was acidified by the addition of HCl (0.5 M). EtOAc (5 mL) was added and the layers were separated. The aqueous layer was extracted twice with EtOAc (2 × 5 mL), and the combined organic extracts were washed with brine, dried, and concentrated under reduced pressure. Purification of the crude product by flash chromatography on silica gel (1:5–3:1 EtOAc/hexane) afforded the desired product 2-(2-benzoylcyclohept-1-en-1-yl)acetic acid (3) (53 mg, 99% yield). ¹H NMR (300 MHz, CDCl₃): δ 7.84 (d, *J* = 7.0 Hz, 2H), 7.60 (t, *J* = 7.4 Hz, 1H), 7.47 (t, *J* = 7.5 Hz, 2H), 3.10 (s, 2H), 2.51–2.43 (m, 4H), 1.86–1.76 (m, 2H), 1.67–1.52 (m, 4H). ¹³C NMR (75 MHz, CDCl₃): δ 202.1 (C), 172.6 (C), 142.4 (C), 135.9 (C), 134.0 (CH), 129.9 (CH), 128.9 (CH), 44.0 (CH₂), 35.7 (CH₂), 32.2 (CH₂), 32.0 (CH₂), 26.5 (CH₂), 25.8 (CH₂). HRMS (APCI-FIA-TOF): *m/z* calculated for C₁₆H₁₉O₃ ([M + H]⁺) 259.1324, found 259.1329.

Procedure for a Large-Scale Catalytic Annulation of 1d. An oven-dried Schlenk tube equipped with a septum and magnetic stirring bar was charged with (*E*)-4-((*S*-phenylpent-4-yn-1-yl)oxy)but-2-enoic acid (500.0 mg, 2.05 mmol), bis(dichloro(pentamethylcyclopentadienyl)rhodium) (32 mg, 0.05 mmol), silver carbonate (850 mg, 3.08 mmol), and DMF (7 mL). The reaction mixture was then stirred at 120 °C. After 24 h, the reaction mixture was concentrated in vacuum. Purification of the crude product by flash chromatography on silica gel (1:10–1:3 EtOAc/hexane) afforded 384 mg of 4-phenyl-3H-furo[3,4-*c*]pyran-6(1H)-one (2d) (77% yield).

Procedure for the Cascade Diels–Alder Reaction. An oven-dried sealed tube equipped with a magnetic stirring bar was charged with *N*-phenylmaleimide (75.2 mg, 0.43 mmol), 1-phenyl-8,9-dihydro-7*H*-pyrano[4,3-*c*]oxepin-3(*5H*)-one (**2d**) (30 mg, 0.12 mmol), and dioxane (1 mL). The reaction mixture was then stirred at 140 °C. After 36 h, the reaction mixture was concentrated in vacuo. Purification of the crude product by flash chromatography on silica gel (1:10–2:1 EtOAc/hexane) afforded the desired product as a white solid (65.5 mg, 97% yield). White solid, mp 249–250 °C. ¹H NMR (300 MHz, CDCl₃): δ 7.51–7.33 (m, 11H), 7.29–7.22 (m, 4H), 4.27 (s, 2H), 3.76 (t, *J* = 6.2 Hz, 2H), 3.69 (t, *J* = 3.0 Hz, 1H), 3.44 (d, *J* = 8.3 Hz, 2H), 3.16 (dd, *J* = 8.3, 3.0 Hz, 2H), 2.54–2.45 (m, 2H), 1.69–1.57 (m, 2H). ¹³C NMR (75 MHz, CDCl₃): δ 175.3 (C), 173.9 (C), 139.1 (C), 139.0 (C), 134.6 (C), 131.6 (C), 131.0 (CH), 129.3 (CH), 128.9 (CH), 127.8 (CH), 126.8 (CH), 126.3 (CH), 71.1 (CH₂), 70.9 (CH₂), 53.8 (C), 48.1 (CH), 44.0 (CH), 37.5 (CH), 30.4 (CH₂), 29.3 (CH₂). HRMS (APCI-FIA-TOF): *m/z* calculated for C₃₃H₂₅N₆O₂ ([*M* + *H*]⁺) 545.2071, found 545.2084.

■ ASSOCIATED CONTENT

Supporting Information

The Supporting Information is available free of charge on the ACS Publications website at DOI: 10.1021/acsomega.9b00022.

Experimental procedures and spectroscopic data for new compounds; CCDC 1885153 and CCDC 1885154 contains the supporting crystallographic data for this paper (PDF)

■ AUTHOR INFORMATION

Corresponding Authors

*E-mail: joseluis.mascareñas@usc.es (J.L.M.).

*E-mail: moises.gulias@usc.es (M.G.).

ORCID

David F. Fernández: 0000-0003-3482-0894

Noelia Casanova: 0000-0001-6881-667X

José Luis Mascareñas: 0000-0002-7789-700X

Moisés Gulías: 0000-0001-8093-2454

Present Address

†Department of Chemistry, University of Cambridge, Lensfield Road, Cambridge CB2 1EW, United Kingdom (N.C.).

Notes

The authors declare no competing financial interest.

■ ACKNOWLEDGMENTS

This work has received financial support from Spanish grants (SAF2016-76689-R, CTQ2016-77047-P, and FPI fellowship to D.F.F.), the Consellería de Cultura, Educación e Ordenación Universitaria (ED431C 2017/19, 2015-CP082, and Centro Singular de Investigación de Galicia acreditación 2016-2019, ED431G/09), the European Regional Development Fund (ERDF), and the European Research Council (Advanced Grant no. 340055). The orfeo-cinca network CTQ2016-81797-REDC is also kindly acknowledged.

■ REFERENCES

(1) Wender, P. A.; Verna, V. A.; Paxton, T. J.; Pillow, T. H. Function-Oriented Synthesis, Step Economy, and Drug Design. *Acc. Chem. Res.* **2008**, *41*, 40–49.

(2) For selected recent reviews of metal-catalyzed C–H functionalizations, see: (a) Yeung, C. S.; Dong, V. M. Catalytic dehydrogenative cross-coupling: forming carbon–carbon bonds by oxidizing two carbon–hydrogen bonds. *Chem. Rev.* **2011**, *111*, 1215–1292. (b) Engle, K. M.; Mei, T.-S.; Wasa, M.; Yu, J.-Q. Weak coordination as a powerful means for developing broadly useful C–H functionalization reactions. *Acc. Chem. Res.* **2012**, *45*, 788–802. (c) Chen, D. Y.-K.; Youn, S. W. C–H activation: a complementary tool in the total synthesis of complex natural products. *Chem. - Eur. J.* **2012**, *18*, 9452–9474. (d) Chen, Z.; Wang, B.; Zhang, J.; Yu, W.; Liu, Z.; Zhang, Y. Transition metal-catalyzed C–H bond functionalization by the use of diverse directing groups. *Org. Chem. Front.* **2015**, *2*, 1107–1295. (e) Gensch, T.; Hopkinson, M. N.; Glorius, F.; Wencel-Delord, J. Mild metal-catalyzed C–H activation: examples and concepts. *Chem. Soc. Rev.* **2016**, *45*, 2900–2936. (f) Sambiagio, C.; Schönbauer, D.; Blicke, R.; Dao-Huy, T.; Pototschnig, G.; Schaaf, P.; Wiesinger, T.; Zia, M. F.; Wencel-Delord, J.; Besset, T.; Maes, B. U. W.; Schnürch, M. A comprehensive overview of directing groups applied in metal-catalyzed C–H functionalisation chemistry. *Chem. Soc. Rev.* **2018**, *47*, 6603–6743.

(3) Peneau, A.; Guillou, C.; Chabaud, L. Recent Advances in [Cp**M*^{III}] (*M* = Co, Rh, Ir)-Catalyzed Intramolecular Annulation Through C–H Activation. *Eur. J. Org. Chem.* **2018**, *2018*, 5777–5794.

(4) For a recent review in the field, see: Gulías, M.; Mascareñas, J. L. Metal-catalyzed annulations through activation and cleavage of C–H bonds. *Angew. Chem., Int. Ed.* **2016**, *55*, 11000–11019.

(5) For selected articles on Rh-catalyzed annulations with alkynes, involving C–H activations, see: (a) Guimond, N.; Gouliaras, C.; Fagnou, K. Rhodium(III)-catalyzed isoquinolone synthesis: the N–O bond as a handle for C–N bond formation and catalyst turnover. *J. Am. Chem. Soc.* **2010**, *132*, 6908–6909. (b) Wang, H.; Grohmann, C.; Nimphius, C.; Glorius, F. Mild Rh(III)-catalyzed C–H activation and annulation with alkyne MIDA boronates: short, efficient synthesis of heterocyclic boronic acid derivatives. *J. Am. Chem. Soc.* **2012**, *134*, 19592–19595. (c) Qi, Z.; Wang, M.; Li, X. Access to indenones by rhodium(III)-catalyzed C–H annulation of aryl nitrones with internal alkynes. *Org. Lett.* **2013**, *15*, 5440–5443. (d) Seoane, A.; Casanova, N.; Quiñones, N.; Mascareñas, J. L.; Gulías, M. Straightforward assembly of benzoxepines by means of a rhodium(III)-catalyzed C–H functionalization of *o*-vinylphenols. *J. Am. Chem. Soc.* **2014**, *136*, 834–837. (e) Seoane, A.; Casanova, N.; Quiñones, N.; Mascareñas, J. L.; Gulías, M. Rhodium(III)-catalyzed dearomatizing (3 + 2) annulation of 2-alkenylphenols and alkynes. *J. Am. Chem. Soc.* **2014**, *136*, 7607–7610. (f) Dateer, R. B.; Chang, S. Selective cyclization of aryl nitrones to indolines under external oxidant-free conditions: dual role of Rh(III) catalyst in the C–H activation and oxygen atom transfer. *J. Am. Chem. Soc.* **2015**, *137*, 4908–4911. (g) Li, S.-S.; Wang, C.-Q.; Lin, H.; Zhang, X.-M.; Dong, L. Rhodium(III)-catalyzed oxidative annulation of 7-azaindoles and alkynes via double C–H activation. *Org. Lett.* **2015**, *17*, 3018–3021. (h) Font, M.; Cendón, B.; Seoane, A.; Mascareñas, J. L.; Gulías, M. Rhodium(III)-catalyzed annulation of 2-alkenyl anilides with alkynes through C–H activation: direct access to 2-substituted indolines. *Angew. Chem., Int. Ed.* **2018**, *57*, 8255–8259. (i) Seoane, A.; Comanescu, C.; Casanova, N.; García-Fandiño, R.; Xabier, D.; Mascareñas, J. L.; Gulías, M. Rhodium-catalyzed annulation of *ortho*-alkenylanilides with alkynes: Formation of unexpected naphthalene adducts. *Angew. Chem., Int. Ed.* **2019**, *58*, 1700–1704.

(6) (a) Ueura, K.; Satoh, T.; Miura, M. Rhodium- and iridium-catalyzed oxidative coupling of benzoic acids with alkynes via regioselective C–H bond cleavage. *J. Org. Chem.* **2007**, *72*, 5362–5367. (b) Ueura, K.; Satoh, T.; Miura, M. An efficient waste-free oxidative coupling via regioselective C–H bond cleavage: Rh/Cu-catalyzed reaction of benzoic acids with alkynes and acrylates under air. *Org. Lett.* **2007**, *9*, 1407–1409. (c) Satoh, T.; Ueura, K.; Miura, M. Rhodium- and iridium-catalyzed oxidative coupling of benzoic acids with alkynes and alkenes. *Pure Appl. Chem.* **2008**, *80*, 1127–1134. (d) Shimizu, M.; Hirano, K.; Satoh, T.; Miura, M. Waste-free synthesis of condensed heterocyclic compounds by rhodium-catalyzed

oxidative coupling of substituted arene or heteroarene carboxylic acids with alkynes. *J. Org. Chem.* **2009**, *74*, 3478. (e) Mochida, S.; Hirano, K.; Satoh, T.; Miura, M. Synthesis of functionalized alpha-pyrone and butenolide derivatives by rhodium-catalyzed oxidative coupling of substituted acrylic acids with alkynes and alkenes. *J. Org. Chem.* **2009**, *74*, 6295–6298. (f) Li, Q.; Yan, Y.; Wang, X.; Gong, B.; Tang, X.; Shi, J.; Xu, H. E.; Yi, W. Water as a green solvent for efficient synthesis of isocoumarins through microwave-accelerated and Rh/Cu-catalyzed C–H/O–H bond functionalization. *RSC Adv.* **2013**, *3*, 23402–23408. (g) Kudo, E.; Shibata, Y.; Yamazaki, M.; Masutomi, K.; Miyauchi, Y.; Fukui, M.; Sugiyama, H.; Uekusa, H.; Satoh, T.; Miura, M.; Tanaka, K. Oxidative annulation of arenecarboxylic and acrylic acids with alkynes under ambient conditions catalyzed by an electron-deficient rhodium(III) complex. *Chem. - Eur. J.* **2016**, *22*, 14190. (h) Liu, X.-G.; Gao, H.; Zhang, S.-S.; Li, Q.; Wang, H. N–O bond as external oxidant in group 9 Cp*M(III)-catalyzed oxidative C–H coupling reactions. *ACS Catal.* **2017**, *7*, 5078–5086. (i) Li, Y.-T.; Zhu, Y.; Tu, G.-L.; Zhang, J.-Y.; Zhao, Y.-S. Rhodium(III)-catalyzed oxidative annulation of acrylic acid with alkynes: An easy approach to the synthesis of α -pyrones. *Chem. - Asian J.* **2018**, *13*, 3281–3284.

(7) For reactions catalyzed by Ru(II), see: (a) Ackermann, L.; Pospech, S.; Graczyk, K.; Rauch, K. Versatile synthesis of isocoumarins and alpha-pyrones by ruthenium-catalyzed oxidative c-h/o-h bond cleavages. *Org. Lett.* **2012**, *14*, 930–933. (b) Deponti, M.; Kozhushkov, S. I.; Yufit, D. S.; Ackermann, L. Ruthenium-catalyzed C-H/O-H and C-H/N-H bond functionalizations: oxidative annulations of cyclopropyl-substituted alkynes. *Org. Biomol. Chem.* **2013**, *11*, 142–148. (c) Warratz, S.; Kornhaas, C.; Cajaraville, A.; Niepötter, B.; Stalke, D.; Ackermann, L. Ruthenium(II)-catalyzed C-H activation/alkyne annulation by weak coordination with O₂ as the sole oxidant. *Angew. Chem., Int. Ed.* **2015**, *54*, 5513–5517. (d) Prakash, R.; Shekarrao, K.; Gogoi, S. Ruthenium(II)-catalyzed alkene C–H bond functionalization on cinnamic acids: a facile synthesis of versatile α -pyrones. *Org. Lett.* **2015**, *17*, 5264–5267. (e) Qiu, Y.; Tian, C.; Massignan, L.; Rogge, T.; Ackermann, L. Electrooxidative ruthenium-catalyzed C–H/O–H annulation by weak *o*-coordination. *Angew. Chem., Int. Ed.* **2018**, *57*, 5818–5822.

(8) For reactions catalyzed by cobalt: (a) Nguyen, T. T.; Grigorjeva, L.; Daugulis, O. Cobalt-catalyzed coupling of benzoic acid C–H Bonds with alkynes, styrenes, and 1,3-dienes. *Angew. Chem., Int. Ed.* **2018**, *57*, 1688–1691. (b) Mandal, R.; Sundararaju, B. Cp*Co(III)-Catalyzed Annulation of Carboxylic Acids with Alkynes. *Org. Lett.* **2017**, *19*, 2544–2547.

(9) Quiñones, N.; Seoane, A.; García-Fandiño, R.; Mascareñas, J. L.; Gulías, M. Rhodium(III)-catalyzed intramolecular annulations involving amide-directed C-H activations: synthetic scope and mechanistic studies. *Chem. Sci.* **2013**, *4*, 2874–2879.

(10) An isolated example of an intramolecular annulation with a benzoic acid derivative has been reported: (a) Wang, Y.; Wang, C.; Wang, Y.; Donga, L.; Sun, J. Total synthesis of Sparstolonin B, a potent anti-inflammatory agent. *RSC Adv.* **2015**, *5*, 12354–12357. For a related process starting from aldehydes, see: (b) Youn, S. W.; Yoo, H. J. One-pot sequential N-heterocyclic carbene/rhodium(III) catalysis: synthesis of fused polycyclic isocoumarins. *Adv. Synth. Catal.* **2017**, *359*, 2176–2183. For selected examples of other types of C–H activation/intramolecular annulation reactions, see: (c) Xu, X.; Liu, Y.; Park, C. M. Rhodium(III)-catalyzed intramolecular annulation through C-H activation: total synthesis of (\pm)-antofine, (\pm)-septicine, (\pm)-tylophorine, and rosettacin. *Angew. Chem., Int. Ed.* **2012**, *51*, 9372–9376. (d) Davis, T. A.; Hyster, T. K.; Rovis, T. Rhodium(III)-catalyzed intramolecular hydroarylation, amidoarylation, and heck-type reaction: three distinct pathways determined by an amide directing group. *Angew. Chem., Int. Ed.* **2013**, *52*, 14181–14185. (e) Shi, Z.; Bouladakis-Arapinis, M.; Koester, D. C.; Glorius, F. Rh(III)-catalyzed intramolecular redox-neutral cyclization of alkenes via C–H activation. *Chem. Commun.* **2014**, *50*, 2650–2652. (f) Tao, P.; Jia, Y. Rhodium-catalyzed intramolecular annulation via C-H activation leading to fused tricyclic indole scaffolds. *Chem. Commun.* **2014**, *50*, 7367–7370. (g) Zhou, B.; Du, J.; Yang, Y.; Li, Y.

Rhodium(III)-catalyzed intramolecular redox-neutral annulation of tethered alkynes: formal total synthesis of (\pm)-goniomitine. *Chem. - Eur. J.* **2014**, *20*, 12768–12772. (h) Zhou, B.; Yang, Y.; Tang, H.; Du, J.; Feng, H.; Li, Y. Rh(III)-catalyzed intramolecular redox-neutral or oxidative cyclization of alkynes: short, efficient synthesis of 3,4-fused indole skeletons. *Org. Lett.* **2014**, *16*, 3900–3903. (i) Song, L.; Tian, G.; He, Y.; Van der Eycken, E. V. Rhodium(III)-catalyzed intramolecular annulation through C-H activation: concise synthesis of rosettacin and oxypalmatine. *Chem. Commun.* **2017**, *53*, 12394–12397. (j) Li, Q.; Li, B.; Wang, B. Rhodium-catalyzed intramolecular cascade sequence for the formation of fused carbazole-annulated medium-sized rings by cleavage of C(sp²)-H/C(sp³)-H bonds. *Chem. Commun.* **2018**, *54*, 9147–9150. (k) Peneau, A.; Retailleau, P.; Guillou, C.; Chabaud, L. Rhodium(III)-catalyzed synthesis of spiro piperidine derivatives via C–H activation. *J. Org. Chem.* **2018**, *83*, 2324–2340.

(11) For an alternative methodology to obtain this type of products through the hydrocarbonation of alkenes, see: Fernández, D. F.; Rodrigues, C. A. B.; Calvelo, M.; Gulías, M.; Mascareñas, J. L.; López, F. Iridium(I)-Catalyzed Intramolecular Cycloisomerization of Enynes: Scope and Mechanistic Course. *ACS Catal.* **2018**, *8*, 7397–7402.

(12) For an example of Diels-Alder/retro Diels-Alder processes in total synthesis involving pyrones, see: Martin, S. F.; Rueger, H.; Williamson, S. A.; Grzejszczak, S. General strategies for the synthesis of indole alkaloids. Total synthesis of (\pm)-reserpine and (\pm)-alpha-yohimbine. *J. Am. Chem. Soc.* **1987**, *109*, 6124–6134.